MOLECULAR AND CELLULAR BIOLOGY, July 2005, p. 5607–5615 Vol. 25, No. 13
0270-7306/05/$08.00+0 doi:10.1128/MCB.25.13.5607–5615.2005

Generation and Characterization of Mice Lacking the Zinc Uptake Transporter ZIP3

Jodi Dufner-Beattie, Zhixin L. Huang, Jim Geiser, Wenhao Xu, and Glen K. Andrews*

Department of Biochemistry and Molecular Biology, University of Kansas Medical Center, Kansas City, Kansas 66160-7421

Received 24 January 2005/Returned for modification 10 March 2005/Accepted 30 March 2005

The mouse *ZIP3* (SLC39A3) gene encodes an eight-transmembrane-domain protein that has been conserved in mammals and can function to transport zinc. To analyze the expression of *ZIP3* in the early embryo and neonate and to determine its in vivo function, we generated *ZIP3* null mice in which the *ZIP3* open reading frame was replaced with that of the enhanced green fluorescent protein (EGFP) reporter. EGFP fluorescence revealed that *ZIP3* was expressed in the inner cell mass of the blastocyst and later during embryonic development in many tissues. Elevated expression was apparent in the embryonic brain and neurotube and neonatal gonads. Homozygous knockout mice were viable and fertile and under normal growth conditions exhibited no obvious phenotypic abnormalities. Deletion of *ZIP3* did not alter zinc homeostasis at the molecular level as assessed by essential metal levels and the expression of zinc-responsive genes. In knockout mice stressed with a zinc-deficient diet during pregnancy or at weaning, a subtle increase in the sensitivity to abnormal morphogenesis of the embryo and to depletion of thymic pre-T cells, respectively, was noted. These results suggest that this protein plays an ancillary role in zinc homeostasis in mice.

Zinc is an essential metal required for the proper function of numerous metalloproteins, where it serves as either a structural or catalytic cofactor (6, 34, 46). Thus, when zinc is present in limiting amounts, it can have devastating effects on living organisms. In mammals, zinc deficiency leads to severe dermatitis, growth retardation, mental disorders, and dysfunction of the immune and reproductive systems (4, 18, 22). High levels of zinc, however, are also deleterious and can lead to cytotoxicity. Therefore, maintaining appropriate zinc levels is of critical importance.

Mammalian zinc homeostasis is achieved by regulating the absorption, excretion, and storage of zinc in response to demand and availability. Under normal, zinc-replete conditions, zinc is absorbed from the diet by enterocytes in the small intestine, and excess zinc is released through the pancreas and small intestine as well as the kidney (21, 31, 42). However, under zinc-deficient conditions, zinc absorption by the small intestine increases, and release from the pancreas and small intestine decreases (21).

At the cellular level, maintaining a constant level of zinc is accomplished through the interplay of proteins involved in zinc export, storage and uptake. Export is achieved by the zinc transporter (ZnT; SLC30A) family of cation diffusion facilitator proteins. These proteins generally contain six predicted transmembrane domains and presumably function as multimers (27). They transport zinc out of the cytoplasm either to the cell exterior or into intracellular compartments. To date, ten members of this family have been described in mammals, and two of these, ZnT1 and ZnT2, are regulated by zinc at the mRNA level (36, 39), while four, ZnT1, ZnT2, ZnT4, and ZnT6, are regulated at the level of subcellular localization (23, 28).

Zinc is bound intracellularly by small cysteine-rich proteins called metallothioneins (MTs) (10). In the mouse, there are four MT family members, and two of these, MT-I and -II, are zinc regulated. In the presence of high zinc, MT-I and -II accumulate due to increased transcription rates. In contrast, under low-zinc conditions, MT levels decrease due to a lower transcription rate and protein destabilization (1). Although *MT* genes are nonessential, they appear to function as a "zinc buffer": they sequester zinc when it is present at high levels, protecting against metal toxicity, and under zinc-limiting conditions provide a labile pool of zinc that can be released for use by other proteins.

Cellular zinc uptake is mediated by the ZRT/IRT-like protein (ZIP) family, also designated solute carrier family 39A (SLC39A), of metal ion transporters (16, 20). Members of this family are found in all phylogenetic classifications, from bacteria to mammals, and they transport metal into the cytoplasm from either the cell exterior or intracellular compartments. ZIP proteins contain eight predicted transmembrane domains, with extracellular amino and carboxyl termini and a histidine-rich intracellular loop located between transmembrane domains 3 and 4 that may bind metal.

The human and mouse genomes each encode 14 ZIP proteins, of which only nine have been characterized in any detail. From these and other experiments, it has become apparent that ZIPs differ in tissue-specific expression, relative expression levels, subcellular localization, metal specificity, and mechanism of regulation. As with ZnTs and MTs, several ZIPs are zinc regulated (40). In the mouse, *ZIP4* mRNA abundance correlates inversely with zinc levels (15), and the subcellular localization of ZIP1, ZIP3, ZIP4, and ZIP5 is responsive to zinc levels (13, 28, 30, 47, 48).

* Corresponding author. Mailing address: Department of Biochemistry and Molecular Biology, Mail Stop 3030, University of Kansas Medical Center, 39th and Rainbow Blvd., Kansas City, KS 66160-7421. Phone: (913) 588-6935. Fax: (913) 588-2711. E-mail: gandrews@kumc.edu.

Based on sequence similarity, the ZIP family can be divided into four subfamilies, I and II, GufA, and LIV-1 (44). Subfamily II contains three members in human and mouse (ZIP1, -2, and -3) that share a conserved 12-amino-acid signature sequence (14). *ZIP1* is expressed at relatively high levels in every tissue examined except pancreas, whereas *ZIP2* and *ZIP3* appear to be more tissue-restricted and expressed at lower levels (14). All three of these family members function to specifically increase the accumulation of zinc when expressed in cultured cells. Zinc uptake by ZIP1 and ZIP2 was only modestly inhibited by other metals, whereas uptake by ZIP3 was inhibited by all metals tested except iron, suggesting that it may function to transport other metals, although zinc appears to be its preferred substrate (14).

Despite the wealth of information that has been gained recently about the ZIP family of proteins from in vitro experiments, very little is known about their in vivo expression, regulation, and function. Herein we report the generation and characterization of mice lacking the ZIP3 (SLC39A3) zinc transporter. In these mice, the *ZIP3* open reading frame was replaced with that of the enhanced green fluorescent protein (EGFP), allowing us to examine temporal and tissue-specific *ZIP3* expression at various stages of development in addition to probing the physiological role of ZIP3 in the intact organism.

MATERIALS AND METHODS

Targeting vector construction. A bacterial artificial chromosome (BAC) clone containing the *ZIP3* gene from the 129/SvJ mouse strain was obtained from Incyte Genomics (Palo Alto, CA) and sequenced by Bruce Roe (University of Oklahoma). The purified BAC was digested, and the fragments were subcloned into pBluescriptII-KS(+) (Stratagene, La Jolla, CA). Subclones were plated and lifted in duplicate onto nylon filters, and those containing the *ZIP3* gene were identified by probing with the *ZIP3* cDNA (14). These subclones were subsequently used to construct the targeting vector.

The 4.15-kb upstream arm of the targeting vector spanned from an XbaI site located approximately 650 bp upstream of exon 1 and extended downstream to the *ZIP3* start codon. An XhoI site that had been introduced immediately downstream of the *ZIP3* start codon by PCR was fused in-frame to the coding region of *EGFP* cDNA from the vector pEGFPKT1loxneo (19) (gift from Mario Cappechi, University of Utah, Salt Lake City). Downstream of the *EGFP* cDNA in this plasmid was a *loxP*-flanked *MC1-neo* cassette (45). The 3.36-kb downstream arm was subcloned downstream of this *MC1-neo* cassette and extended from an XbaI site located approximately 600 bp 3′ of exon 4 and extended to a downstream BglII site. This targeting construct was inserted into the XbaI and BglII sites of 4317G9 (gift from Richard Palmiter, University of Washington, Seattle) which are flanked by herpes simplex virus thymidine kinase and diphtheria toxin negative selectable markers.

Homologous recombination of the targeting vector into the endogenous locus results in the insertion of two novel EcoRI sites, allowing the targeted and wild-type alleles to be distinguished by Southern blotting using both 5′- and 3′-flanking probes. The 5′-flanking probe is a 463-bp BglII-BglII genomic fragment that recognizes a ≈19.7-kb EcoRI fragment corresponding to the wild-type allele which decreases in size to ≈7.8 kb following homologous recombination. The 3′-flanking probe is an 886-bp XhoI-XbaI genomic fragment that recognizes a 19.7-kb fragment corresponding to the wild-type allele that decreases in size to 7.3 kb following homologous recombination.

Targeted disruption of the *ZIP3* gene in embryonic stem cells. The targeting vector was linearized within the vector backbone with AscI and electroporated into R1 embryonic stem (ES) cells using an ECM 600 electroporator (BTX, San Diego, CA). Colonies were selected with 300 μg/ml G418 (Mediatech, Herndon, VA) and 2 μM ganciclovir (Roche Pharmaceuticals, Nutley, NJ). Selection against diphtheria toxin requires no drug treatment.

Homologous recombinants were screened for by Southern blotting using the 463-bp 5′-flanking probe. Positive clones were subsequently screened with (i) the 886-bp 3′-flanking probe, (ii) a Y-chromosome-specific probe derived from pY2 (35), and (iii) a *neo* cDNA to detect the presence of a single homologously targeted *MC1-neo* cassette.

Generation of *ZIP3* knockout mice. Chimeric mice were generated by microinjection of three independent $ZIP3^{+/-}$ ES cell clones into 3.5-day-old C57BL/6 blastocysts, followed by transfer to pseudopregnant CD-1 foster mothers. Resulting male chimeric mice were mated with C57BL/6 females (Harlan, Indianapolis, IN). Germ line transmission was confirmed by PCR from tail DNA of agouti offspring. As expected, approximately 50% of the agouti pups were heterozygous for the *ZIP3* knockout allele. The PCR screen utilized a set of three primers: mZIP3WT(S) (5′-CATCAGATCCTCTGGAACTGGAGTTACA-3′), mZIP3WT(AS)2 (5′-AACACACAGAGTATGGATTCTCAGAACCC-3′), and neoKO(AS) (5′-GAATGGGCTGACCGCTTCCTC-3′). The mZIP3WT(S) primer was specific for the deleted region of *ZIP3* and detected only the wild-type allele. The NeoKO(S) primer was specific for the *neo* cDNA and detected only the mutant allele. The mZIP3WT(AS) primer detected both the wild-type and mutant alleles. The PCR product for the mutant allele was 326 bp, whereas the product for the wild-type allele was 461 bp. Results from the PCR screen were initially confirmed by Southern blot analysis. Agouti offspring heterozygous for the *ZIP3* knockout allele were bred with C57BL/6 mice. The heterozygous offspring of that mating were inbred to yield wild-type and homozygous *ZIP3* knockout mice.

Animal care and use. Experiments involving mice were performed in accordance with the guidelines from the National Institutes of Health for the care and use of animals and were approved by the Institutional Animal Care and Use Committee. Mouse diets were purchased from Harlan Teklad (Madison, WI) and were identical except for zinc levels, which were as follows: zinc-deficient diet, 1 ppm zinc; zinc-adequate diet, 50 ppm zinc.

To examine *ZIP3*, *ZIP4*, and metallothionein (*MT-I*) expression and to determine tissue levels of essential metals (Zn, Cu, and Fe), adult mice (six per group) were maintained on a zinc-adequate diet and sacrificed, and the indicated tissues were harvested and frozen in liquid nitrogen for subsequent extraction of RNA or for inductively coupled plasma-atomic emission spectrometry (ICP-AES), respectively. Prior to RNA extraction, the indicated tissues from each mouse were pooled. To monitor EGFP fluorescence, indicated tissues or embryos at various stages of development were collected and examined immediately by fluorescence microscopy.

The effect of zinc deficiency during pregnancy on morphogenesis and growth of the embryo was assessed by subjecting pregnant mice to dietary zinc deficiency under the experimental conditions described previously (15). Female mice were mated, and the day a vaginal plug was found was considered day 1 of pregnancy. On day 1, mice were placed in cages and provided free access to zinc-adequate feed and deionized distilled water. On day 8 of pregnancy, mice were placed in pairs in cages with stainless steel false bottoms to reduce the recycling of zinc (9). In addition, water was provided in bottles that had been washed in 4 M HCl and rinsed with deionized water to remove zinc. At this time, the diet was changed to the zinc-deficient feed. On day 14 of pregnancy, the embryos were collected, examined for gross morphological defects, and weighed.

The effect of initiating zinc deficiency at birth was determined by culling litters to eight pups per dam at birth and placing the dams on either a zinc-adequate or zinc-deficient diet. Each dam (six per treatment group) was individually weighed daily up to 5 days, and pups were weighed as litters daily up to 5 days, and an average weight per pup was calculated.

The effect of zinc deficiency at weaning was determined by placing 21-day-old male and female weanlings (approximately equal numbers) on either a zinc-deficient or zinc-adequate diet for 3 weeks. Mice were weighed on days 0, 7, 14, and 21 to determine an average weight per treatment group. On day 21, mice were either put on a zinc-adequate diet to examine recovery or sacrificed to determine average testicular weight, thymus weight, and the distribution of thymocyte subtypes using flow cytometry.

Southern blot analysis. Genomic DNA (1 to 10 μg) extracted from either duplicate ES cell colonies or tail DNA preparations was digested overnight with EcoRI, resolved on 0.7% Tris-acetate-EDTA-agarose gels, transferred to Zeta-Probe GT membranes (Bio-Rad, Hercules, CA), and hybridized overnight using UltraHyb ultrasensitive hybridization buffer (Ambion, Austin, TX) and washed according to the manufacturer's directions. DNA fragments used as probes to detect the *ZIP3* gene, *neo* cDNA, and Y chromosome repetitive elements were excised from parental plasmids and labeled with [^{32}P]dCTP to a minimum specific activity of 10^9 cpm/μg using the random primers DNA labeling system (Invitrogen, Carlsbad, CA). The *neo* probe was hybridized and washed at 38°C due to the high A:T content of the cDNA.

Northern blot analysis. Total RNA was isolated using Trizol reagent (Invitrogen) according to the manufacturer's instructions. RNA (3 μg) was resolved on agarose-formaldehyde gels, transferred to nylon membranes, immobilized via

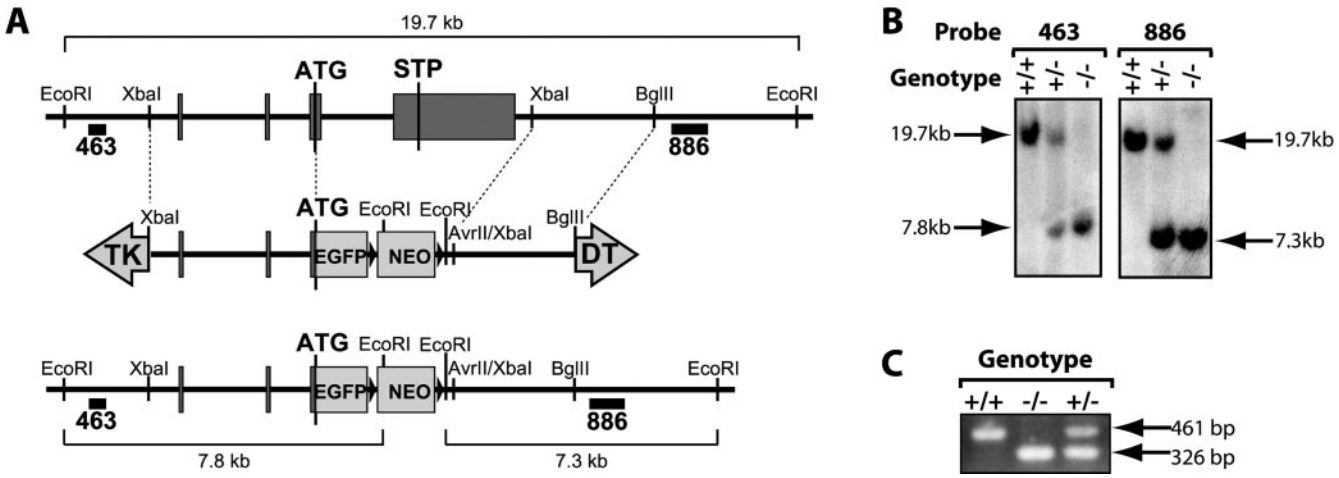

FIG. 1. Targeted disruption of the *ZIP3* gene. (A) Targeting strategy. The gene structure for the *ZIP3* wild-type allele (top) is shown with the four exons (dark gray boxes), the initiator methionine (ATG) and stop (STP) codons, and pertinent restriction sites. The dark horizontal bars represent the locations of the 463-bp 5′-flanking probe and the 886-bp 3′-flanking probe. Targeting vector (middle): herpes simplex virus thymidine kinase (TK); diphtheria toxin (DT); enhanced green fluorescent protein (EGFP) reporter (light gray box); neomycin (Neo). Structure of the targeted mutant allele (bottom). (B) Southern blot genotype analysis of mouse tail DNA. Genomic DNA from wild-type (+/+), heterozygous knockout (+/−), and homozygous knockout (−/−) mice was digested with EcoRI and analyzed by Southern blot analysis using the 5′-flanking probe (463) or 3′-flanking probe (886). (C) PCR genotyping of mouse DNA. Genomic DNA was PCR amplified with a set of three primers to distinguish wild-type from mutant alleles. Amplification of the wild-type allele produces a 461-bp fragment, whereas amplification of the mutant allele produces a 326-bp fragment.

UV cross-linking, and hybridized and washed under stringent conditions as previously described (11, 12, 14, 36). Hybrids were detected by autoradiography with intensifying screens at −80°C. DNA fragments used as probes to detect the *ZIP3* and *ZIP4* cDNAs were excised from parental plasmids and labeled with [^{32}P]dCTP using the random primers DNA labeling system (Invitrogen) as described previously (14, 15). The *MT-I* probe was generated by in vitro transcription as previously described (11). Mouse brain Northern blots were purchased from Panomics (Redwood City, CA).

Fluorescence imaging. EGFP fluorescence was monitored in freshly collected tissue using a Leica DM4000 B microscope (North Central Instruments, Inc., Plymouth, MN).

Trace metal determination. Accumulation of zinc, copper, and iron in the testes (six pairs per group) was determined by inductively coupled plasma-atomic emission spectrometry (ICP-AES) (performed by Jeffrey F. Harper, Scripps Research Institute, La Jolla, CA). Each sample was normalized to magnesium prior to determining average metal levels.

Flow cytometry. Flow cytometric analysis of thymocyte subtypes was performed as previously described (25). Each thymus was passed through a 70-μm cell strainer (BD Biosciences, San Diego, CA) with phosphate-buffered saline containing 2% fetal bovine serum, and the single-cell suspension was reconstituted at a density of 2×10^{10} cells/liter. An aliquot of 10^6 cells was incubated in the presence of 10 μg rat immunoglobulin to block nonspecific binding, followed by incubation with anti-CD4-phycoerythrin (PE) and anti-CD8-fluorescein isothiocyanate (FITC) antibodies (BD Biosciences) for 30 min on ice. The labeled samples were then washed with phosphate-buffered saline containing 2% fetal bovine serum and 1 mg/ml sodium azide and suspended in 1 ml of 2% formaldehyde in phosphate-buffered saline to fix the cells. Samples were analyzed using a Beckman Coulter EPICS XL-MCL fluorescence activated cell sorter (Miami, FL) by exciting the fluorochromes at 488 nm and detecting PE and FITC emissions at 575 and 530 nm, respectively. Data from at least 10,000 events were acquired from each sample.

Statistics. The experimental data for trace metals were evaluated by Student's *t* test. The remaining data were analyzed by one-way analysis of variance with post hoc Turkey's comparisons using the SAS System version 8 (SAS Institute, Cary, NC). Data are presented as means ± standard deviation or standard error of the mean. Differences between groups were considered significant at $P < 0.05$.

RESULTS

Generation of *ZIP3* knockout mice. Mice with a targeted disruption of the *ZIP3* gene were generated by homologous recombination in embryonic stem (ES) cells. The targeting construct fused the initiator methionine codon of *ZIP3* with the open reading frame of the enhanced green fluorescent protein (EGFP) reporter while deleting the remainder of the *ZIP3* open reading frame (Fig. 1A). This allowed for *EGFP* expression that was driven by the *ZIP3* promoter in targeted cells. A *loxP*-flanked *neo* cassette located downstream of the *EGFP* cDNA was used for positive selection (19), and the flanking thymidine kinase and diphtheria toxin cassettes were used for negative selection. Homologous recombinants were identified by Southern blot analysis of EcoRI-digested genomic DNA. The 463-bp 5′-flanking probe recognized a 19.7-kb EcoRI fragment that decreased in size to 7.8 kb following targeting (Fig. 1A and B). Similarly, the 886-bp 3′-flanking probe recognized the same 19.7-kb EcoRI fragment that decreased in size to 7.3 kb following targeting. A PCR screen was designed to allow rapid genotyping of mice (Fig. 1C). PCR genotyping data were initially compared with the Southern blot genotyping data and gave identical results.

Successful knockout of *ZIP3* was confirmed using two additional assays. First, since *ZIP3* mRNA is highly abundant in the testes (14), Northern blot analysis was carried out using testes RNA from mice of different *ZIP3* genotypes. As expected, *ZIP3* mRNA was abundant in wild-type mice, undetectable in *ZIP3* homozygous knockout mice, and present at intermediate levels in *ZIP3* heterozygous knockout mice (Fig. 2A). Second, since the *ZIP3* open reading frame was replaced with that of the EGFP reporter in the targeted *ZIP3* gene, EGFP fluorescence was used to monitor *ZIP3* expression. Testes were collected from mice of different genotypes and analyzed by fluorescence microscopy. Testes from wild-type adult mice (Fig. 2B) showed a low level of autofluorescence. In contrast, homozygous knockout mice showed a high level of EGFP fluorescence, and heterozygous knockout mice showed intermedi-

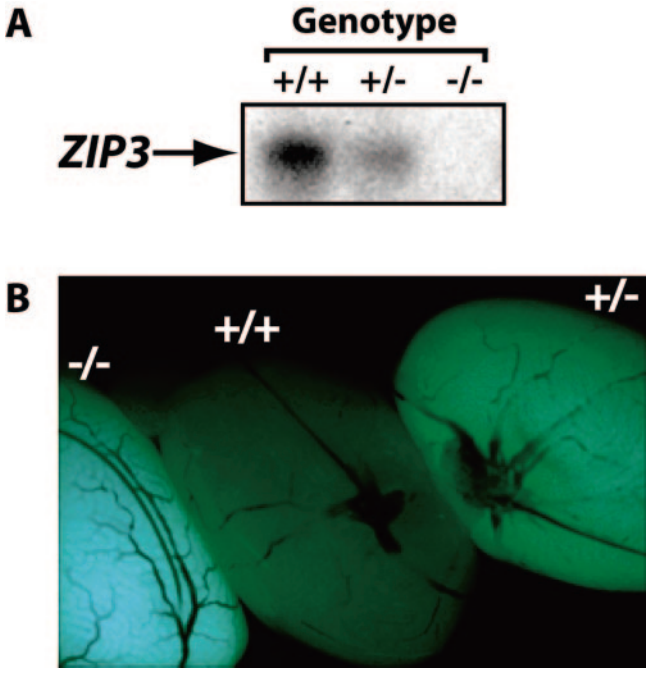

FIG. 2. Confirmation of targeted disruption of *ZIP3*. (A) Northern blot analysis of *ZIP3* expression in testes. Total RNA was isolated from the testes of wild-type (+/+), heterozygous knockout (+/−), and homozygous knockout (−/−) mice and analyzed by Northern blot analysis using a *ZIP3*-specific cDNA probe. (B) EGFP expression in the testes. Testes were collected from wild-type (+/+), heterozygous knockout (+/−), and homozygous knockout (−/−) adult mice and examined immediately by microscopy for EGFP fluorescence.

ate levels. Thus, EGFP fluorescence appears to provide a semiquantitative measure of *ZIP3* expression in terms of gene dosage.

Monitoring *ZIP3* expression in the embryo and neonate by detecting EGFP. Using EGFP as a measure of *ZIP3* expression, expression patterns during embryonic development were examined. Blastocysts from either wild-type matings or homozygous *ZIP3* knockout matings were collected on day 4 of development, just before implantation, and mixed together in equal numbers. Side-by-side comparisons of wild-type versus homozygous knockout blastocysts revealed elevated EGFP fluorescence specifically in the inner cell mass of homozygous knockout blastocysts (Fig. 3A). Thus, *ZIP3* is expressed very early during development of the mouse embryo.

ZIP3 expression was then examined on embryonic days 11 and 14. Heterozygous *ZIP3* knockout embryos collected on day 11 exhibited ubiquitous EGFP fluorescence (Fig. 3B). Ubiquitous fluorescence was also detected on day 14 (Fig. 3C). However, EGFP fluorescence was exceptionally strong in the developing central nervous system on day 14 (Fig. 3D). Neonatal mice were also examined, and EGFP fluorescence was exceptionally strong in the ovary and testes (data not shown). This suggested that *ZIP3* expression is higher in testes, ovary, and the developing nervous system relative to other tissues. Previous Northern blot analysis of adult tissue RNAs is consistent with this finding, which indicates that these expression patterns are initiated during development and maintained into adulthood (14).

To further examine *ZIP3* expression in the adult brain, Northern blot analysis of polyadenylated RNA isolated from various regions of the brain was performed. *ZIP3* mRNA was detected in all brain regions examined, and its abundance in all regions was relatively equal (data not shown). Overall, these results establish that the mouse *ZIP3* gene is activated before implantation and is expressed in many embryonic cell types but displays elevated expression in the gonads and central nervous system.

Effects of *ZIP3* knockout on essential metal levels and zinc-responsive gene expression. To determine whether targeted deletion of the *ZIP3* gene alters zinc homeostasis, two functional assays were carried out. First, zinc content in the testes was determined by inductively coupled plasma-atomic emission spectrometry. Zinc levels in the testes from homozygous knockout mice were identical to those in wild-type mice (Fig. 4A). In addition, neither copper nor iron levels were different between knockout and wild-type mice. Second, the effect of *ZIP3* knockout on zinc-responsive gene expression was assessed by Northern blotting. The small intestine and testes were collected from mice of different genotypes and analyzed for the expression of two known zinc-responsive genes, *MT-I* and *ZIP4*. *MT-I* mRNA is depleted, whereas *ZIP4* mRNA is enriched in intestinal RNA from zinc-deficient mice (15). In both tissues, *MT-I* gene expression did not differ significantly between wild-type, heterozygous knockout, and homozygous knockout mice (Fig. 4B). Likewise, *ZIP4* expression in the intestine did not differ between genotypes (Fig. 4B) and, consistent with previous findings (15), was not detectable in the testes. Furthermore, the subcellular localization of ZIP4 was examined in the intestine and visceral yolk sac, which was previously demonstrated to be on the apical surface of enterocytes and endoderm cells under conditions of zinc deficiency (15). No ZIP4 was detected on the apical surfaces of these cells in the *ZIP3* knockout mice fed a zinc-adequate diet (data not shown).

Immortalized *ZIP3* knockout mouse embryonic fibroblasts were examined for *MT-I* regulation. No detectable differences between wild-type and knockout cells were observed in dose-response, time course, or levels of *MT-I* mRNA induction in response to zinc (data not shown). These data all indicate that at the molecular level, deletion of the *ZIP3* gene does not appreciably affect zinc status in unstressed mice.

Phenotypic analysis of *ZIP3* knockout mice. *ZIP3* homozygous knockout mice were generated from heterozygous matings at the expected Mendelian ratio. They were fertile and appeared normal, with no discernible differences between homozygous knockout mice and their wild-type littermates over several generations in terms of body mass and reproductive success, as measured by rate of pregnancy and litter size (data not shown). Given the absence of an obvious phenotype in *ZIP3* knockout mice under normal animal husbandry conditions, mice were subjected to dietary zinc deficiency using several different protocols.

Since *ZIP3* is expressed at highest levels in the testes, it seemed likely that a phenotype would be most evident in this tissue. Adult male mice were placed on a zinc-deficient diet for 8 weeks, and their testes were collected and analyzed. There was no difference in testicular weight between wild-type and

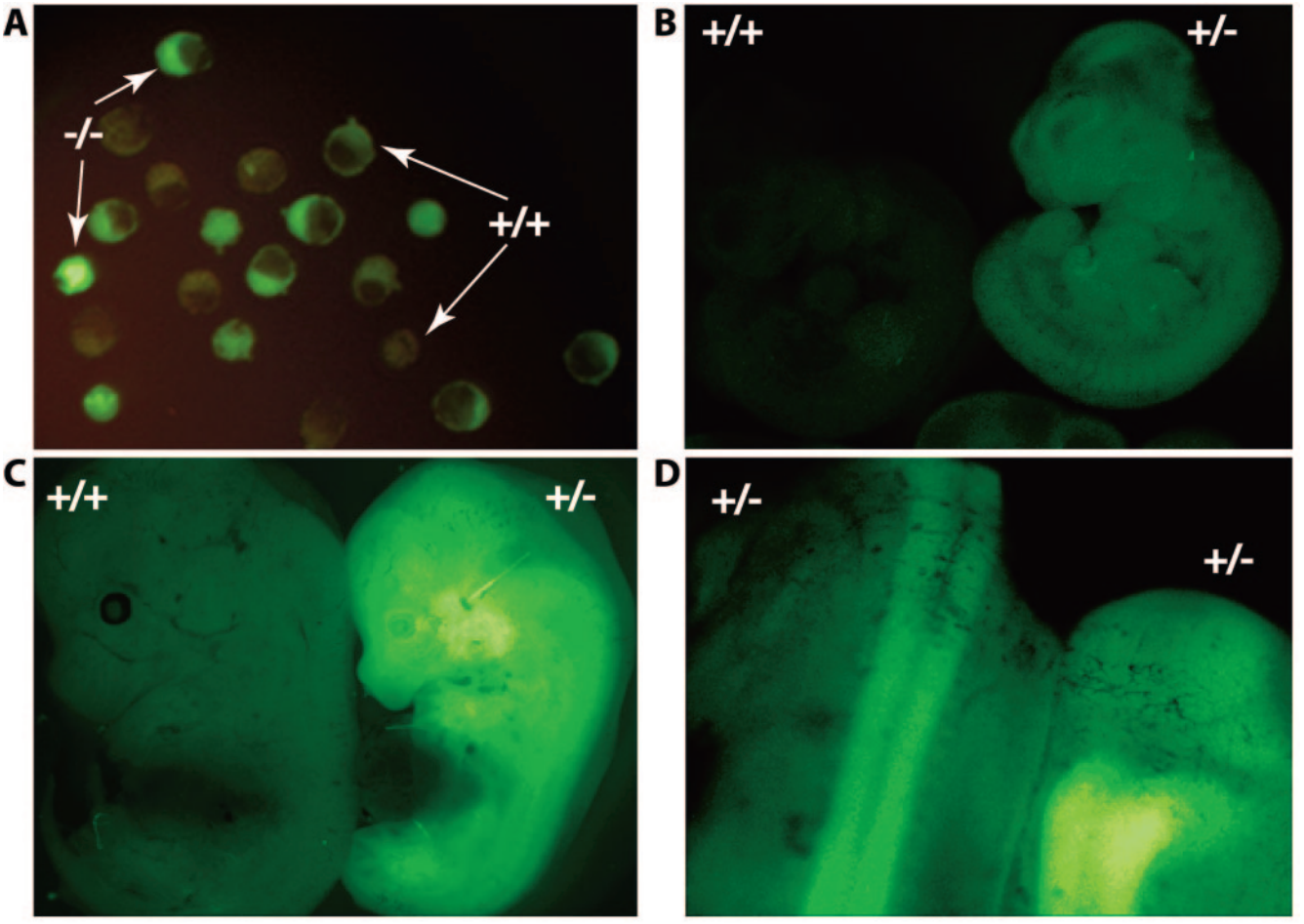

FIG. 3. Detection of *ZIP3* expression patterns by EGFP fluorescence in mouse embryos. (A) Blastocysts from wild-type and homozygous knockout matings were collected on day 4 from the uteri of pregnant mice and compared side by side using fluorescence microscopy to detect EGFP. Arrowheads demarcate either homozygous knockout (−/−) or wild-type (+/+) blastocysts. Wild-type (+/+) and heterozygous knockout (+/−) embryos were analyzed by fluorescence microscopy for EGFP on day 11 (B) and day 14 (C and D) of gestation.

knockout mice, and testes from knockout mice appeared histologically normal (data not shown).

Zinc deficiency during pregnancy provides a model system with which to examine the effects of zinc on embryonic development. The demand for zinc by developing embryos increases during midgestation, coincident with a phase of rapid growth. Superimposing zinc deficiency during this period accentuates the demand for zinc and causes retarded growth, delayed development, and embryonic lethality (2, 11, 38). To determine whether deletion of *ZIP3* causes more severe defects during pregnancy under zinc-deficient conditions, mice were fed either a zinc-adequate or zinc-deficient diet beginning on day 8 of pregnancy. On day 14, the mice were sacrificed, and embryos were collected, weighed, and observed for morphological abnormalities (Table 1). Consistent with previous findings, dietary zinc deficiency caused approximately 25% of the embryos from wild-type matings to develop abnormally. Abnormal embryos were significantly smaller than their morphologically normal littermates. Although paternal *ZIP3* knockout had no effect on the size or number of the abnormal embryos, there was a small increase in the percentage of abnormal embryos in mothers that lacked *ZIP3*, and this effect was exacerbated if the embryos also lacked functional *ZIP3*. Thus, under these experimental conditions, a minor increase in susceptibility to zinc deficiency during pregnancy correlated with loss of function of *ZIP3*.

ZIP3 expression has been reported in the mammary gland during lactation (28) and was recently shown to facilitate zinc import into the mouse mammary epithelial cell line HC11 (29). Based on these findings, it was postulated that ZIP3 plays a critical role in transferring zinc from the maternal circulation into the milk to ensure optimal zinc concentrations for the suckling neonate. To test this hypothesis, the effects of maternal dietary zinc deficiency on growth of the suckling neonate was examined. On the day of birth, dams were fed either a zinc-adequate or zinc-deficient diet. Pups that suckled from dams fed the zinc-adequate diet showed significant weight gain compared to pups of the corresponding genotype that suckled from dams fed the zinc-deficient diet for 5 days (Fig. 5A). However, there was no significant difference within each dietary group between wild-type and knockout pups. By day 10, several of the neonatal pups had died regardless of genotype (data not shown). Analysis of the dams' body weight revealed that, regardless of genotype, dams maintained on a zinc-ade-

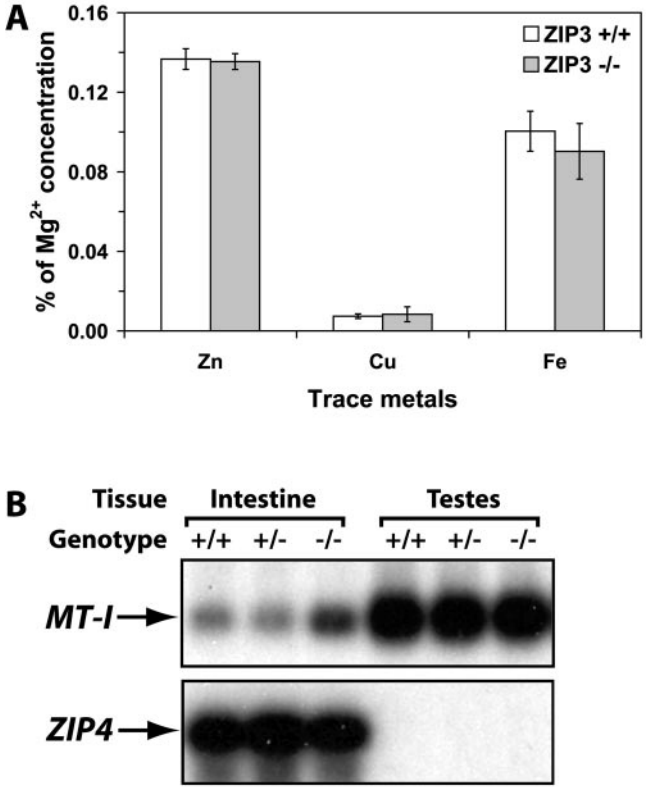

FIG. 4. Effect of targeted deletion of the *ZIP3* gene on levels of essential metals and expression of zinc-responsive genes. (A) Effect of *ZIP3* deletion on trace metal levels in the testes. Wild-type (+/+) or homozygous knockout (−/−) adult mice were maintained on a zinc-adequate diet, and testes were collected and analyzed by inductively coupled plasma-atomic emission spectrometry (ICP-AES) for zinc (Zn), copper (Cu), and iron (Fe) levels. Individual samples were normalized to magnesium, and bars represent the mean of normalized samples ($n = 6$) ± 1 standard deviation. (B) Effect of *ZIP3* deletion on mRNA levels of zinc-responsive genes. Total RNA was isolated from the intestine and testes of wild-type (+/+), heterozygous knockout (+/−), and homozygous knockout (−/−) adult mice and analyzed by Northern blot hybridization using the *MT-I* (top) or *ZIP4* (bottom) probe.

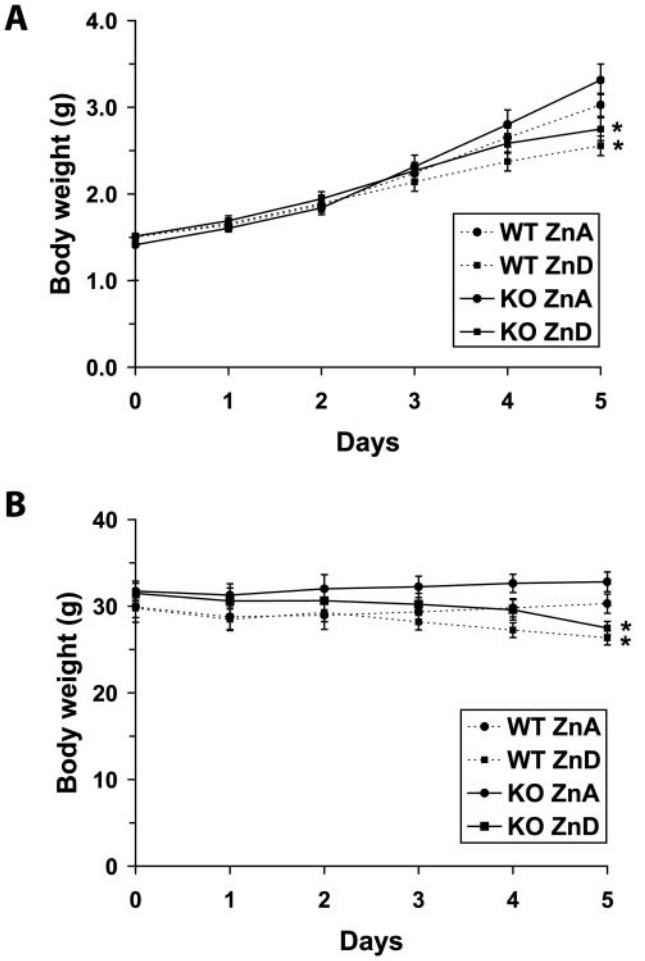

FIG. 5. Effect of initiating maternal zinc deficiency at birth on neonatal growth of *ZIP3* knockout mice. On the day of birth, pups from either wild-type (WT, dotted line) or homozygous knockout (KO, solid line) matings were culled to eight per litter, and dams were placed on either a zinc-adequate (ZnA, ●) or zinc-deficient (ZnD, ■) diet. Pups (A) and dams (B) were weighed daily for 5 days to determine an average weight per animal for each treatment group. Data points represent means ($n = 4$ to 6) ± standard error of the mean (error bars). * denotes a significant difference between the zinc-adequate and zinc-deficient diets on day 5 ($P \leq 0.05$) for each genotype.

quate diet showed no change in body weight over the 5-day duration of the experiment (Fig. 5B). In contrast, both wild-type and knockout dams maintained on zinc-deficient diets showed a decrease in body weight over the time course of the experiment.

TABLE 1. Effect of zinc deficiency during pregnancy[a]

Parent genotype		Progeny genotype	No. of embryos	% Abnormal	Average wt (mg)	
Female	Male				Normal	Abnormal
+/+	+/+	+/+	100	23	155 ± 10	90 ± 14
+/+	−/−	+/−	80	25	140 ± 13	100 ± 13
−/−	+/+	+/−	54	30	140 ± 13	100 ± 15
−/−	−/−	−/−	93	36	156 ± 15	92 ± 16

[a] Mice were fed a zinc-deficient diet beginning on day 8 of pregnancy, and embryos were collected and weighed on day 14. Embryos were scored as abnormal if they showed signs of growth retardation or limb bud and craniofacial defects.

Finally, the effect of initiating a zinc-deficient diet at weaning, a period of rapid growth, was examined. Weanlings were placed on either a zinc-adequate or zinc-deficient diet, and changes in the average body weight for each animal were determined over time. Growth curves for wild-type and *ZIP3* homozygous knockout mice were nearly identical: weanlings that were maintained on a zinc-adequate diet demonstrated increases in body weight which began to plateau by 21 days, whereas those maintained on a zinc-deficient diet showed no change in body weight over the duration of the experiment (Fig. 6A). In addition, when zinc was replenished in the diet of zinc-deficient mice on day 21, there was no significant difference in growth recovery between wild-type and knockout mice.

In parallel experiments, zinc-deficient mice were sacrificed on day 21, and the testes and thymus were collected and weighed. Regardless of the *ZIP3* genotype, testes from mice

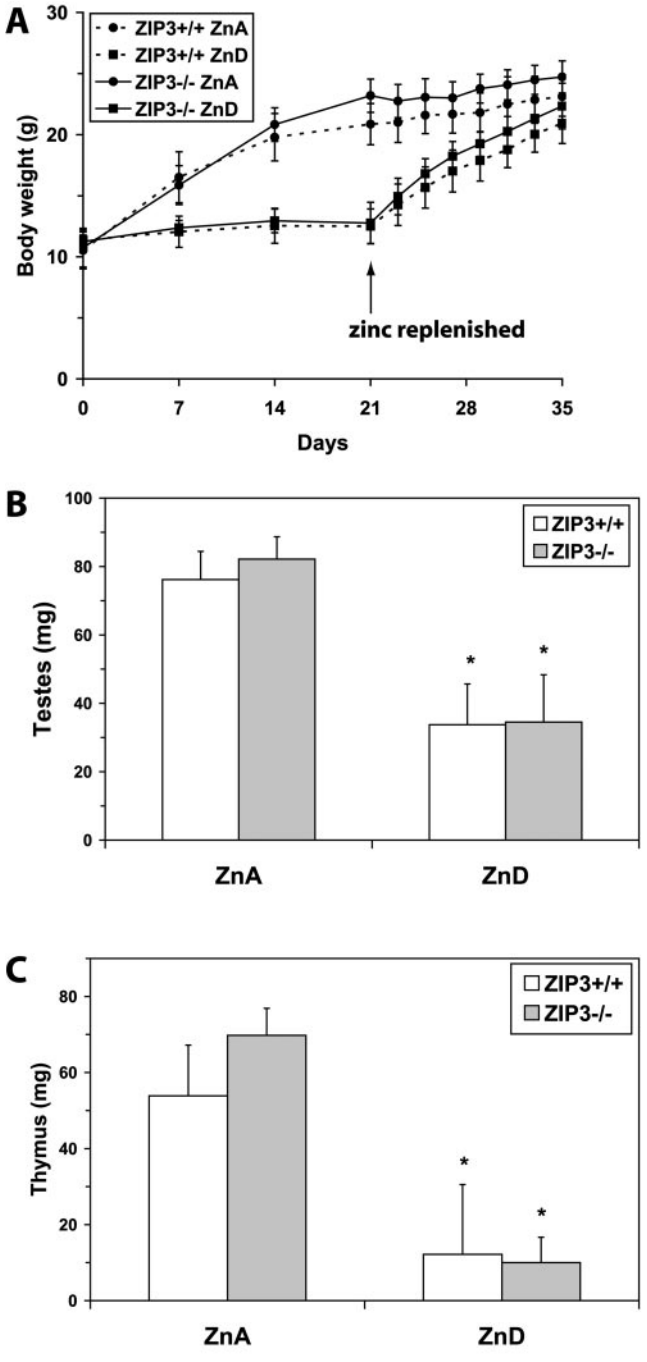

FIG. 6. Effect of initiating zinc deficiency at weaning on body, testicular, and thymic weight in *ZIP3* knockout mice. On day 21 after birth, wild-type (+/+) and homozygous knockout (−/−) pups were weaned and then fed either a zinc-adequate (ZnA, ●) or zinc-deficient (ZnD, ■) diet. (A) On days 7, 14, and 21 of the diet, pups were weighed, and an average wet weight was determined. On day 21 of the diet, zinc was replenished by feeding the zinc-adequate diet, and pups were weighed daily during recovery. (Only every other day is shown graphically.) In parallel experiments, day 21 zinc-deficient mice were sacrificed, and the testes (B) and thymuses (C) were harvested and weighed. Data are represented as the mean ± standard deviation (error bars) ($n = 12$ to 26 for A and C and $n = 7$ to 17 for B). * denotes a significant difference between the zinc-adequate and zinc-deficient diets ($P \leq 0.05$).

TABLE 2. Effect of zinc deficiency on distribution of T-cell subpopulations[a]

Treatment group and genotype	T-cell subpopulations (% of total per thymus ± SEM)			
	$CD4^-$ $CD8^-$ (pro-T cells)	$CD4^+$ $CD8^-$ (helper T cells)	$CD4^+$ $CD8^+$ (pre-T cells)	$CD4^-$ $CD8^+$ (cytolytic T cells)
Zinc-adequate diet				
+/+	2.7 ± 0.3	15.8 ± 1.1	76.7 ± 1.7	4.8 ± 0.5
−/−	2.1 ± 0.3	11.8 ± 0.7	81.2 ± 1.2	4.9 ± 0.4
Zinc-deficient diet				
+/+	7.7 ± 1.3	21.7 ± 1.8	61.5 ± 3.7	9.1 ± 1.0
−/−	8.0 ± 1.4	38.2 ± 3.9	35.2 ± 6.3	18.6 ± 2.2

[a] Thymic cells obtained from mice fed a zinc-adequate or zinc-deficient diet for 21 days were collected and analyzed for CD4 and CD8 T-cell markers.

maintained on a zinc-adequate diet weighed twofold more than testes from mice maintained on a zinc-deficient diet (Fig. 6B). Similar results were seen for the thymuses except that there was a sixfold difference in weight between thymuses derived from zinc-adequate animals and those derived from zinc-deficient animals (Fig. 6C). Again, these weights were unaffected by *ZIP3* genotype.

Previous studies have shown that thymic atrophy is a hallmark of zinc deficiency and is associated with substantially reduced numbers of pre-T lymphocytes due to enhanced apoptosis of this T-cell subpopulation (17, 32). Pro-T cells and helper and cytolytic T cells survive zinc deficiency better and therefore become a higher proportion of the remaining thymocyte population. To determine whether *ZIP3* knockout alters the thymocyte profile during zinc deficiency, thymocytes were isolated and sorted by flow cytometry using antibodies against CD4 and CD8 markers. As expected, zinc deficiency resulted in a significant decrease in the percentage of pre-T lymphocytes ($CD4^+$ $CD8^+$) and a concomitant increase in the pro-T cells ($CD4^-$ $CD8^-$) and the cytolytic and helper T cells ($CD4^-CD8^+$ and $CD4^+$ $CD8^-$, respectively) in wild-type mice (Table 2). This loss of pre-T lymphocytes was significantly accentuated in knockout mice. Under zinc-adequate conditions, thymocyte subpopulation profiles were similar between wild-type and knockout mice, the only difference being a slight decrease in helper T cells ($CD4^+$ $CD8^-$) with a concomitant increase in pre-T cells ($CD4^+$ $CD8^+$) in knockout mice relative to wild-type mice.

DISCUSSION

The ZIP superfamily of integral membrane proteins includes members from all phyla that function to transport metals, including zinc, iron, manganese, and possibly others, into the cytoplasm either from the cell exterior or from intracellular compartments. We previously characterized ZIP3 as a member of subfamily II of the mammalian ZIPs. Subfamily II consists of three members (ZIP1 to ZIP3) that are structurally related and that have been highly conserved between mice and humans. Each of these proteins can function to preferentially transport zinc into transfected cells (14), but little is known about the physiological roles that each of these proteins (ZIP1 to ZIP3) may play in maintaining metal homeostasis in vivo. The experiments presented here describe the targeted deletion of *ZIP3* and replacement of its open reading frame with that of

EGFP. This approach allowed us to examine temporal- and tissue-specific expression patterns of *ZIP3* and to assess the function of ZIP3 in the mouse.

Our previous studies of the expression of mouse *ZIP3* demonstrated that this mRNA is detectable at very low levels in many adult tissues but is particularly abundant in the testes and less so in the brain and ovaries (14). Information from public databases suggests that *ZIP3* is expressed in a wide array of tissues and cell types. The abundance of this mRNA does not appear to be regulated by dietary zinc in mice. Analysis of EGFP fluorescence in the *ZIP3* knockout mice was consistent with these findings. Fluorescence was intense in the adult and neonatal gonads but was also strong in the developing neurotube and brain and ubiquitous at low levels throughout the embryo at various stages of development. Remarkably, *ZIP3* expression occurs very early during development and was clearly detectable in the inner cell mass at the blastocyst stage before implantation. Despite this, *ZIP3* does not appear to exert an essential function during early development. In contrast, two *ZIP* genes have recently been shown to play an essential role during development in lower eukaryotes. The *fear of intimacy gene* in *Drosophila melanogaster* is required for formation of the embryonic gonad and respiratory system (41), and the zebrafish *LIV-1* gene is essential for proper gastrulation (49). Both of these genes belong to the LIV-1 subfamily.

Mice lacking the ZIP3 transporter exhibited no obvious phenotypic abnormality under normal growth conditions and were only slightly more susceptible to the effects of dietary zinc deficiency. Although it is possible that the function of ZIP3 was not revealed by the experiments that were performed, a number of different hallmarks of zinc deficiency were measured in both embryos and adults. It is unclear why we did not see a more dramatic effect on neonatal growth in light of the recent findings by Kelleher et al. (29), which suggest that ZIP3 plays a major role in zinc uptake into mammary epithelial cells. This may reflect the limitations associated with the in vitro system used in those studies or a compensatory mechanism in the knockout mice.

The lack of a significant phenotype in these knockout mice may reflect functional redundancy between members of subfamily II of the mouse ZIPs. ZIPs 1, 2, and 3 are strikingly similar in structure (14). Their genes each contain four exons, and the encoded peptides share 41 to 48% amino acid similarity. These similarities suggest that these genes may have arisen from a single gene, and based on this, it could be postulated that they now serve redundant functions. Consistent with this concept, each of these ZIP proteins exhibit similar kinetic parameters of zinc transport. However, *ZIP1* mRNA is far more abundant than *ZIP2* or *ZIP3* mRNAs, and the *ZIP1* gene is expressed in essentially every organ and cultured cell that has been examined. Functional redundancy within this family would not be unexpected, given the critical importance of zinc in so many biological processes.

Alternatively, the lack of a strong phenotype seen in *ZIP3* knockout mice may reflect functional redundancy between ZIP proteins from different subfamilies. Although ZIP proteins from different subfamilies are divergent, it remains possible that they do perform overlapping functions. It is known that there are at least two zinc uptake transporters that can function to absorb dietary zinc in enterocytes of the small intestine. Mammalian ZIP4, a member of the LIV-1 subfamily, is involved in zinc uptake in enterocytes and embryonic visceral endoderm cells where it responds to changes in zinc levels at both the level of mRNA abundance and subcellular localization (15). Mutations in *ZIP4* cause acrodermatitis enteropathica, a rare genetic disorder of zinc uptake in humans. However, dietary zinc supplementation can suppress the symptoms of this disease (5, 7, 33, 37, 43), suggesting the presence of additional zinc transport mechanisms in the intestine. Our studies demonstrated that *ZIP1* and *ZIP3* are also expressed in the intestine and embryonic visceral endoderm, and results reported herein suggest that ZIP3 plays an ancillary role in dietary zinc absorption.

Loss of ZIP3 function may also be compensated for by other proteins that are involved in zinc homeostasis. It is known that the metallothioneins (MTs), which chelate zinc, as well as zinc exporters (ZnT; SLC30 family), which remove zinc from the cytoplasm, are responsive to zinc status (1). *MT-I* and *-II* mRNA and protein abundance correlates directly with zinc levels, and several ZnTs respond to zinc at the level of mRNA abundance and protein subcellular localization. Thus, the ability of these proteins to respond to changes in zinc levels may allow cells to accommodate the loss of zinc uptake that occurs in the absence of ZIP3. Interestingly, deletions in many of these genes cause more severe phenotypes than that seen with *ZIP3*. Deletion of the *MT-I* and *-II* genes renders mice more susceptible to the effects of zinc deficiency (2), whereas overexpression of MT-I dramatically protects mice from these effects (11). Targeted deletion of *ZnT1* results in early embryonic lethality in homozygous knockout mice (3). Mice that lack ZnT3 are prone to seizures elicited by kainic acid treatment (8), and homozygous deletion of *ZnT5* results in poor growth, osteopenia, low body fat, muscle weakness, and male-specific cardiac death (26). In addition, the naturally occurring lethal milk mouse carries a nonsense mutation in the *ZnT4* gene (24). These mice produce zinc-deficient milk and thus cause zinc deficiency in nursing pups. Clearly, each of the above-mentioned genes plays an important physiological role in mammalian zinc homeostasis.

The question remains why deletion of *ZIP3* causes only a subtle phenotype while mutation of other genes involved in zinc homeostasis causes more profound effects. Whether functional redundancy between ZIP family members, compensation between different classes of proteins involved in zinc homeostasis, or a combination of these contribute to the lack of overt phenotype seen in ZIP3-deficient mice remains to be determined. Knockout experiments to test for functional redundancy are under way.

ACKNOWLEDGMENTS

This work was funded, in part, by NIH grant DK50181 to G.K.A. Z.L.H. was supported, in part, by a Biomedical Research Fellowship from KU Medical Center.

We thank Mario Cappechi for the pEGFPKT1loxneo vector and Richard Palmiter for the 4317G9 vector, Alan Godwin and Ken Peterson for technical advice, Bill Justice for help with the flow cytometric analyses, and Gary Lin and Michael Leins for technical assistance. We also thank members of the Transgenic and Gene-Targeting Institutional Facility (TGIF) at the KU Medical Center for the generation of targeted ES cell clones and blastocyst injection.

REFERENCES

1. **Andrews, G. K.** 1990. Regulation of *metallothionein* gene expression. Prog. Food Nutr. Sci. **14:**193–258.
2. **Andrews, G. K., and J. Geiser.** 1999. Expression of *metallothionein-I and -II* genes provides a reproductive advantage during maternal dietary zinc deficiency. J. Nutr. **129:**1643–1648.
3. **Andrews, G. K., H. Wang, S. K. Dey, and R. D. Palmiter.** 2004. The mouse *zinc transporter* 1 gene provides an essential function during early embryonic development. Genesis **40:**74–81.
4. **Apgar, J.** 1985. Zinc and reproduction. Annu. Rev. Nutr. **5:**43–68.
5. **Baudon, J. J., J. L. Fontaine, M. Larregue, G. Feldmann, and R. Laplane.** 1978. Acrodermatitis enteropathica. Anatomo-clinical study of 2 familial cases treated with zinc sulfate. Arch. Fr. Pediatr. **35:**63–73.
6. **Berg, J. M., and Y. G. Shi.** 1996. The galvanization of biology: A growing appreciation for the roles of zinc. Science **271:**1081–1085.
7. **Bohane, T. D., E. Cutz, J. R. Hamilton, and D. G. Gall.** 1977. Acrodermatitis enteropathica, zinc, and the Paneth cell. A case report with family studies. Gastroenterology **73:**587–592.
8. **Cole, T. B., C. A. Robbins, H. J. Wenzel, P. A. Schwartzkroin, and R. D. Palmiter.** 2000. Seizures and neuronal damage in mice lacking vesicular zinc. Epilepsy Res. **39:**153–169.
9. **Cook Mills, J. M., and P. J. Fraker.** 1993. Functional capacity of the residual lymphocytes from zinc-deficient adult mice. Br. J. Nutr. **69:**835–848.
10. **Coyle, P., J. C. Philcox, L. C. Carey, and A. M. Rofe.** 2002. Metallothionein: the multipurpose protein. Cell. Mol. Life Sci. **59:**627–647.
11. **Dalton, T. P., K. Fu, R. D. Palmiter, and G. K. Andrews.** 1996. Transgenic mice that over-express metallothionein-I resist dietary zinc deficiency. J. Nutr. **126:**825–833.
12. **Dalton, T. P., R. D. Palmiter, and G. K. Andrews.** 1994. Transcriptional induction of the mouse *metallothionein-I* gene in hydrogen peroxide-treated Hepa cells involves a composite major late transcription factor/antioxidant response element and metal response promoter elements. Nucleic Acids Res. **22:**5016–5023.
13. **Dufner-Beattie, J., Y. M. Kuo, J. Gitschier, and G. K. Andrews.** 2004. The adaptive response to dietary zinc in mice involves the differential cellular localization and zinc-regulation of the zinc transporters ZIP4 and ZIP5. J. Biol. Chem. **279:**49082–49090.
14. **Dufner-Beattie, J., S. J. Langmade, F. Wang, D. Eide, and G. K. Andrews.** 2003. Structure, function, and regulation of a subfamily of mouse zinc transporter genes. J. Biol. Chem. **278:**50142–50150.
15. **Dufner-Beattie, J., F. Wang, Y. M. Kuo, J. Gitschier, D. Eide, and G. K. Andrews.** 2003. The acrodermatitis enteropathica gene *ZIP4* encodes a tissue-specific, zinc-regulated zinc transporter in mice. J. Biol. Chem. **278:** 33474–33481.
16. **Eide, D.** 1997. Molecular biology of iron and zinc uptake in eukaryotes. Curr. Opin. Cell Biol. **9:**573–577.
17. **Fraker, P. J., and L. E. King.** 2004. Reprogramming of the immune system during zinc deficiency. Annu. Rev. Nutr. **24:**277–298.
18. **Fraker, P. J., L. E. King, T. Laakko, and T. L. Vollmer.** The dynamic link between the integrity of the immune system and zinc status. J. Nutr. **130:** 1399S–1406S, 2000.
19. **Godwin, A. R., H. S. Stadler, K. Nakamura, and M. R. Capecchi.** 1998. Detection of targeted *GFP-Hox* gene fusions during mouse embryogenesis. Proc. Natl. Acad. Sci. USA **95:**13042–13047.
20. **Guerinot, M. L.** 2000. The ZIP family of metal transporters. Biochim. Biophys. Acta **1465:**190–198.
21. **Hambidge, M., and N. F. Krebs.** 2001. Interrelationships of key variables of human zinc homeostasis: Relevance to dietary zinc requirements. Annu. Rev. Nutr. **21:**429–452.
22. **Harris, E. D.** 2002. Cellular transporters for zinc. Nutr. Rev. **60:**121–124.
23. **Huang, L., C. P. Kirschke, and J. Gitschier.** 2002. Functional characterization of a novel mammalian zinc transporter, ZnT6. J. Biol. Chem. **277:** 26389–26395.
24. **Huang, L. P., and J. Gitschier.** 1997. A novel gene involved in zinc transport is deficient in the lethal milk mouse. Nat. Genet. **17:**292–297.
25. **Huang, Z. L., and P. J. Fraker.** 2003. Chronic consumption of a moderately low protein diet does not alter hematopoietic processes in young adult mice. J. Nutr. **133:**1403–1408.
26. **Inoue, K., K. Matsuda, M. Itoh, H. Kawaguchi, H. Tomoike, T. Aoyagi, R. Nagai, M. Hori, Y. Nakamura, and T. Tanaka.** 2002. Osteopenia and male-specific sudden cardiac death in mice lacking a zinc transporter gene, Znt5. Hum. Mol. Genet. **11:**1775–1784.
27. **Kambe, T., Y. Yamaguchi-Iwai, R. Sasaki, and M. Nagao.** 2004. Overview of mammalian zinc transporters. Cell. Mol. Life Sci. **61:**49–68.
28. **Kelleher, S. L., and B. Lonnerdal.** 2003. Zn transporter levels and localization change throughout lactation in rat mammary gland and are regulated by Zn in mammary cells. J. Nutr. **133:**3378–3385.
29. **Kelleher, S. L., and B. Lonnerdal.** 2005. Zip3 plays a major role in zinc uptake into mammary epithelial cells and is regulated by prolactin. Am. J. Physiol. Cell. Physiol. **288:**1042–1047.
30. **Kim, B. E., F. D. Wang, J. Dufner-Beattie, G. K. Andrews, D. J. Eide, and M. J. Petris.** 2004. Zn^{2+}-stimulated endocytosis of the mZIP4 zinc transporter regulates its location at the plasma membrane. J. Biol. Chem. **279:** 4523–4530.
31. **King, J. C., D. M. Shames, and L. R. Woodhouse.** 2000. Zinc homeostasis in humans. J. Nutr. **130**(Suppl.)**:**1360S–1366S.
32. **King, L. E., and P. J. Fraker.** 2002. Zinc deficiency in mice alters myelopoiesis and hematopoiesis. J. Nutr. **132:**3301–3307.
33. **Krieger, I., G. W. Evans, and P. S. Zelkowitz.** 1982. Zinc dependency as a cause of chronic diarrhea in variant acrodermatitis enteropathica. Pediatrics **69:**773–777.
34. **Krishna, S. S., I. Majumdar, and N. V. Grishin.** 2003. Structural classification of zinc fingers. Nucleic Acids Res. **31:**532–550.
35. **Lamar, E. E., and E. Palmer.** 1984. Y-encoded, species-specific DNA in mice: evidence that the Y chromosome exists in two polymorphic forms in inbred strains. Cell **37:**171–177.
36. **Langmade, S. J., R. Ravindra, P. J. Daniels, and G. K. Andrews.** 2000. The transcription factor MTF-1 mediates metal regulation of the mouse *ZnT1* gene. J. Biol. Chem. **275:**34803–34809.
37. **Larregue, M., J. J. Baudon, J. L. Fontaine, G. Feldmann, and R. Laplane.** 1977. Acrodermatitis enteropathica: zinc sulfate therapy. Ann. Dermatol. Venereol. **104:**737–744.
38. **Lee, D. K., J. Geiser, J. Dufner-Beattie, and G. K. Andrews.** 2003. Pancreatic metallothionein-l may play a role in zinc homeostasis during maternal dietary zinc deficiency in mice. J. Nutr. **133:**45–50.
39. **Liuzzi, J. P., R. K. Blanchard, and R. J. Cousins.** 2001. Differential regulation of zinc transporter 1, 2, and 4 mRNA expression by dietary zinc in rats. J. Nutr. **131:**46–52.
40. **Liuzzi, J. P., and R. J. Cousins.** 2004. Mammalian zinc transporters. Annu. Rev. Nutr. **24:**151–172.
41. **Mathews, W. R., F. Wang, D. J. Eide, and M. Van Doren.** 2005. Drosophila *fear of intimacy* encodes a Zrt/IRT-like protein (ZIP) family zinc transporter functionally related to mammalian ZIP proteins. J. Biol. Chem. **280:**787–795.
42. **McClain, C. J.** 1990. The pancreas and zinc homeostasis. J. Lab. Clin. Med. **116:**275–276.
43. **Ohlsson, A.** 1981. Acrodermatitis enteropathica Reversibility of cerebral atrophy with zinc therapy. Acta Paediatr. Scand. **70:**269–273.
44. **Taylor, K. M., and R. I. Nicholson.** 2003. The LZT proteins; the *LIV-1* subfamily of zinc transporters. Biochim. Biophys. Acta **1611:**16–30.
45. **Thomas, K. R., and M. R. Capecchi.** 1987. Site-directed mutagenesis by gene targeting in mouse embryo-derived stem cells. Cell **51:**503–512.
46. **Vallee, B. L., and D. S. Auld.** 1990. Zinc coordination, function, and structure of zinc enzymes and other proteins. Biochemistry **29:**5647–5659.
47. **Wang, F., J. Dufner-Beattie, B. E. Kim, M. J. Petris, G. Andrews, and D. J. Eide.** 2004. Zinc-stimulated endocytosis controls activity of the mouse ZIP1 and ZIP3 zinc uptake transporters. J. Biol. Chem. **279:**24631–24639.
48. **Wang, F., B. E. Kim, M. J. Petris, and D. J. Eide.** 2004. The mouse ZIP5 protein functions as a zinc transporter and localizes to the basolateral surface of polarized cells. J. Biol. Chem. **279:**51433–51441.
49. **Yamashita, S., C. Miyagi, T. Fukada, N. Kagara, Y. S. Che, and T. Hirano.** 2004. Zinc transporter LIVI controls epithelial-mesenchymal transition in zebrafish gastrula organizer. Nature **429:**298–302.